Biochimica et Biophysica Acta 1837 (2014) 287–295

Contents lists available at ScienceDirect

Biochimica et Biophysica Acta

journal homepage: www.elsevier.com/locate/bbabio

Redox-Optimized ROS Balance and the relationship between mitochondrial respiration and ROS

Sonia Cortassa, Brian O'Rourke, Miguel A. Aon *

Division of Cardiology, Johns Hopkins University School of Medicine, Baltimore, MD, USA

ARTICLE INFO

Article history:
Received 9 August 2013
Received in revised form 7 November 2013
Accepted 11 November 2013
Available online 20 November 2013

Keywords:
Redox environment
Forward electron transport
NADH
GSH
H_2O_2
Mild uncoupling

ABSTRACT

The Redox-Optimized ROS Balance [R-ORB] hypothesis postulates that the redox environment [RE] is the main intermediary between mitochondrial respiration and reactive oxygen species [ROS]. According to R-ORB, ROS emission levels will attain a minimum vs. RE when respiratory rate (VO_2) reaches a maximum following ADP stimulation, a tenet that we test herein in isolated heart mitochondria under forward electron transport [FET]. ROS emission increased two-fold as a function of changes in the RE (~400 to ~900 mV·mM) in state 4 respiration elicited by increasing glutamate/malate (G/M). In G/M energized mitochondria, ROS emission decreases two-fold for RE ~500 to ~300 mV·mM in state 3 respiration at increasing ADP. Stressed mitochondria released higher ROS, that was only weakly dependent on RE under state 3. As a function of VO_2, the ROS dependence on RE was strong between ~550 and ~350 mV·mM, when VO_2 is maximal, primarily due to changes in glutathione redox potential. A similar dependence was observed with stressed mitochondria, but over a significantly more oxidized RE and ~3-fold higher ROS emission overall, as compared with non-stressed controls. We conclude that under non-stressful conditions mitochondrial ROS efflux decreases when the RE becomes less reduced within a range in which VO_2 is maximal. These results agree with the R-ORB postulate that mitochondria minimize ROS emission as they maximize VO_2 and ATP synthesis. This relationship is altered quantitatively, but not qualitatively, by oxidative stress although stressed mitochondria exhibit diminished energetic performance and increased ROS release.

1. Introduction

How mitochondria attain a reliable energy provision while keeping ROS within physiological limits compatible with signaling is a relevant question linked with the relationship between respiration and ROS. The importance of this question cannot be overstated because of the central role that mitochondrial energetics/redox functions play in the pathogenesis of numerous human disorders [reviewed in [1,2]]. Also unbeknownst to us is how the dependence of ROS emission on respiration is influenced by oxidative stress. This is also a fundamental question because it is becoming increasingly clear that mitochondrial dysfunction under oxidative stress underlies aging [3,4] and acute or chronic disease conditions such as metabolic disorders (obesity, diabetes) [5], cancer [6,7], neurodegeneration [8], and cardiovascular disease [9–11]. The role of mitochondrial functions pertains not only to pathology but also to vital physiological activities, such as exercise and nutrition [12].

"Uncoupling to survive" [13], or its parental "mild uncoupling" [MU] [14,15], and the recent Redox-Optimized ROS Balance [R-ORB] [16], are hypotheses attempting to explain at a mechanistic level the link between mitochondrial respiration and ROS levels. A main difference between MU and R-ORB is the proposed intermediary between respiration and ROS: mitochondrial membrane potential [$\Delta\Psi_m$] and redox environment [RE], respectively.

The MU hypothesis postulates that in energized mitochondria, mild uncoupling, i.e. slight drop in $\Delta\Psi_m$, decreases mitochondrial ROS production. Originally, it was proposed that MU was mediated by proteins that regulate the proton permeability of inner mitochondrial membrane [15,17]. Evidence of mild-uncoupling has been obtained in isolated mitochondria under both forward [18] and reverse electron transport modes of respiration [14]. In this hypothetical framework, $\Delta\Psi_m$ would be the main mediator between the rate of respiration and ROS. That a slight decrease in $\Delta\Psi_m$ should also decrease ROS is a major prediction of the MU hypothesis but this has been verified only in isolated mitochondria, not in intact cells [16]. Indeed, MU elicited an increase rather than a decrease in ROS in living cardiomyocytes from guinea pig loaded with two ROS probes simultaneously. The R-ORB hypothesis was introduced in part to account for this discrepancy.

Abbreviations: ARed, Amplex Red; $\Delta\Psi_m$, mitochondrial membrane potential; FET, forward electron transport; G/M, glutamate/malate; GSH, reduced glutathione; GSSG, oxidized form of GSH; H_2O_2, hydrogen peroxide; LS, light scattering; MCB, monochlorobimane; MU, mild uncoupling; OxPhos, oxidative phosphorylation; RE, redox environment; R-ORB, Redox-Optimized ROS Balance; ROS, reactive oxygen species; Trx, thioredoxin; VO_2, respiratory rate

* Corresponding author at: Johns Hopkins University, Division of Cardiology, 720 Rutland Avenue, Ross Bldg. 1059, Baltimore, MD 21205, USA. Tel.: 410 955 2759; fax: 410 502 5055.
E-mail address: maon1@jhmi.edu (M.A. Aon).

0005-2728/$ – see front matter © 2013 Elsevier B.V. All rights reserved.
http://dx.doi.org/10.1016/j.bbabio.2013.11.007

The R-ORB hypothesis postulates that [16]: *i*) the extent of ROS imbalance is determined by the RE; *ii*) ROS levels attain a minimum at intermediate values of RE; *iii*) ROS overflow can occur at both extremes of RE, i.e. highly reduced or highly oxidized, but through completely different mechanisms [Fig. 1]. According to R-ORB, the net flux of ROS released from mitochondria depends upon ROS production by the respiratory chain and ROS scavenging, the balance of which is altered at both extremes of RE. When very reduced [Fig. 1, right hand arm], the RE corresponds to slow electron flow through the respiratory chain thus increasing the probability of generating the free radical superoxide, irrespective of high antioxidant availability. Instead, when the RE is rather oxidized [Fig. 1, left hand arm], the compromised scavenging capacity becomes rate-controlling, thus ROS overflow occurs.

Another major difference between MU and R-ORB concerns the consequences on mitochondrial energetics. To decrease ROS levels, MU proposes uncoupling, i.e. decreasing $\Delta\Psi_m$, the main driving force for ATP synthesis and ion and substrate movement in mitochondria. This mainly applies to fully energized mitochondria, i.e. close to state 4, where $\Delta\Psi_m$ is maximal and according to MU more prone to produce ROS. In contrast, with its focus on the RE, R-ORB predicts that ROS emission levels will reach a minimum when mitochondria maximize their energetic output [i.e. maximal state 3 respiration] which corresponds to more oxidized values of RE, as compared with the low respiratory flux in state 4. Thus, R-ORB encompasses both states 4 and 3 of respiration and, potentially, includes MU [Fig. 1, right branch of red curve] in a more encompassing view.

In the present work, we test whether mitochondrial ROS emission levels tend to a minimum when respiration attains a maximum, a major tenet of the R-ORB hypothesis. This question begs the dual functional role of mitochondria comprising consistency in energy supply and tuning of ROS to non-harming levels, compatible with signaling. Moreover, we also put to test the postulate that ROS imbalance depends on the RE, in this case changed as a function of respiratory substrates and ADP. We perform these studies with isolated guinea pig heart mitochondria in the absence or the presence of oxidative stress.

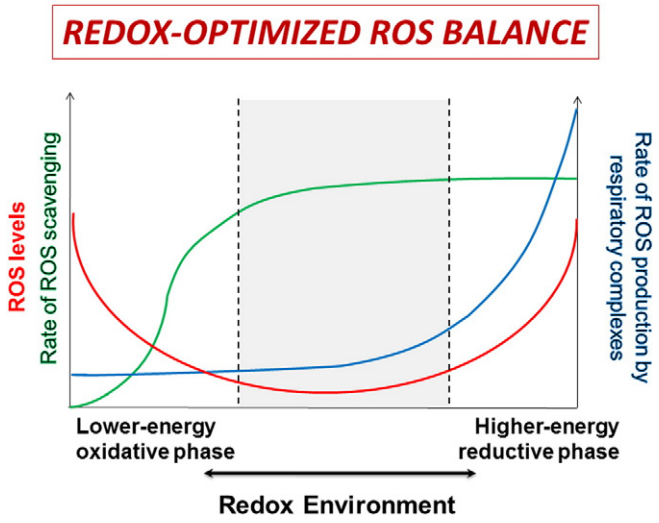

Fig. 1. The Redox-Optimized ROS Balance [R-ORB] hypothesis. R-ORB postulates that ROS levels [as the net result of production and scavenging] depend on the intra-cellular and -mitochondrial RE. It also proposes that there is a minimum level of ROS emission when mitochondria maximize their energetic output. According to R-ORB, a decrease in ROS levels does not require compromising the efficiency of mitochondrial energy transduction [e.g. mild $\Delta\Psi_m$ uncoupling] but instead it proposes that under high energy demand, and despite large respiratory rates, ROS emission levels will be kept to a minimum by ROS scavenging systems. Recently, this contention received experimental support [20]. Physiological ROS signaling [denoted between dashed lines] occurs within a range close to the minimum of the overall [red] curve that corresponds to intermediate values of the RE. Oxidative stress can happen at either extreme of RE, either highly reduced or highly oxidized, but governed by completely different mechanisms.
Reprinted by permission from Aon, Cortassa, O'Rourke (2010) Biochim Biophys Acta 1797, 865–877.

2. Materials and methods

2.1. Mitochondrial isolation

Procedures for the isolation and handling of mitochondria from guinea pig heart were performed as described [16,19]. Respiratory Control Ratios [state 3/state 4 respirations with 5 mM glutamate + malate] of 8 or higher were obtained using this method.

2.2. Assay of mitochondrial respiration

Freshly isolated mitochondria were assayed for respiration as described [20]. Briefly, a high throughput automated 96-well extracellular flux analyzer [Seahorse Bioscience XF96, Billerica, MA] was utilized, and a medium [buffer B] containing [in mM]: 137 KCl, 2 KH_2PO_4, 0.5 EGTA, 2.5 $MgCl_2$, 20 HEPES at pH 7.2 and 37 °C, in the presence of 0.2% fatty acid free BSA. Respiration was evaluated with substrates of complex I [glutamate/malate, G/M, 5 mM each]. Mitochondrial protein was determined using the bicinchronic acid method, BCA™ protein assay kit [Thermo Scientific, IL]. VO_2 was determined in parallel with the same mitochondrial preparation utilized for the fluorescent determination of other redox and energetic variables.

2.3. Other bioenergetic variables and ROS detection

NAD[P]H, hydrogen peroxide [H_2O_2], GSH, 90° light scattering, and $\Delta\Psi_m$ were determined as described [16,19], and monitored simultaneously with a wavelength scanning fluorometer [Quantamaster, Photon Technology, Inc.] utilizing the same medium above for measuring respiration [excluding BSA], and a multidye program for simultaneous online monitoring of different fluorescent probes. H_2O_2 was detected using the Amplex Red kit from Invitrogen [Carlsbad, CA].

2.4. Estimation of the redox environment [RE]

The RE comprises two factors, the half-cell reduction potential [Nernst potential, see Eq. (2) below] of the redox couple *i*, *Ei*, e.g. $NADH/NAD^+$, and the concentration of the reduced species *i* of that couple, e.g. NADH. The RE is calculated according to [21,22]:

$$Redox\,environment = \sum_{i=1}^{n} E_i[reduced\,species]_i \quad (1)$$

Eq. (1) represents the summation of the product of the redox potential times the concentration of the reduced species of the linked redox couples present in the system. Redox couples include those involved in electron transport [$NADH/NAD^+$] and in antioxidant pathways [$NADPH/NADP^+$, GSH/GSSG, $Trx[SH]_2$/TrxSS]. In this work, we will estimate the RE as a function of $NADH/NAD^+$ and GSH/GSSG redox couples.

In the mitochondrial matrix, NADH at ~1 mM and GSH at 1–2 mM represent the two major redox couples contributing to the RE, as compared with ~0.1 mM NADPH and ~0.01–0.05 mM Trx [20,22–24].

2.5. Redox potential determination

The Nernst equation was used to estimate the redox potential of each redox couple. This equation relates the change in free energy of the transfer of electrons to the voltage of an electrochemical cell, and can be expressed as:

$$\Delta E = \Delta E^{\circ} - \frac{R\,T}{n\,F} ln\,Q. \quad (2)$$

$\Delta E°$ is the electromotive force under standard conditions that corresponds to the difference in standard reduction potentials of the two half-cells involved in the process; n is the number of electrons exchanged in the chemical process; F is the Faraday constant; R, the universal gas constant; T, temperature (Kelvin scale). Q stands for the quotient of the concentration of reduced over oxidized species from the redox couple. Standard redox potentials, $\Delta E°$ [see Eq. (2)], used were −320 mV for NADH/NAD^+ and −240 mV for 2 GSH/GSSG [21].

To calculate the redox potential using Eq. (2) we need to determine the redox status of the couple, i.e. the relative concentration of reduced and oxidized species.

2.6. NAD(P)H and GSH determination

NAD(P)H was monitored by exciting mitochondrial suspensions at 340 nm and collecting the emission at 450 nm. The NAD(P)H signal was calibrated with addition of 1 mM KCN [100%] and 6 μM FCCP [0% ± 5%–10%] at the end of the experiment [e.g. Fig. 2B]. Under certain experimental conditions FCCP addition may only account for 90% to 95% of NAD(P)H due to the existence of NADPH and bound-NADH; the latter may vary between mitochondrial preparations within the specified range and may imply longer time to achieve full oxidation.

GSH was quantitated in supernatants from mitochondria undergoing state 4 and 3 respirations after trichloroacetic acid precipitation as described elsewhere [24]. Briefly, after neutralizing to pH 7.4 the trichloroacetic acid supernatants, we utilized non-enzymatic fluorescent labeling of thiols with the probe *N*-[4-[7-diethylamino-4-methylcoumarin-3-yl] phenyl]maleimide; picomole levels of GSH can be detected with this method [24]. The rate of reaction of the thiol fluorescent probe with GSH is linear within the range of 20–100 pmol [see [24], for further details]. We determined values ranging between 2.0 and 1.0 mM GSH for control, and 1.0 to 0.5 mM GSH for stressed mitochondria from guinea pig heart. The matrix concentration of GSH was estimated considering a mitochondrial volume of 2 μl/mg of mitochondrial protein according to our previous determination [19]. A 1 to 2 mM mitochondrial matrix GSH pool appears reasonable considering the 2.7 mM intracellular GSH determined before in guinea pig ventricular cardiomyocytes [25].

GSH was also monitored as glutathione S-bimane, GSB [λ_{exc} = 390 nm; λ_{em} = 480 nm]. GSB is the fluorescent adduct obtained after the reversible reaction of monochlorobimane, MCB, with GSH catalyzed by glutathione S-transferase [26,27] in mitochondria loaded with 20 μM MCB, as described [16].

Knowing the relative (%) value of NAD(P)H or the GSH concentration, and the total pool of each one of them present in the mitochondrial matrix, the concentration value (in mM) of each species can be estimated under specified conditions. In this work, we assumed 1 mM for the total pool of NADH, and determined 2 mM or 1 mM for GSH under control, non-stressed, or stressed conditions, respectively (see below). The values of RE reported herein (e.g. Fig. 6) are in agreement with values obtained by computational modeling [21].

2.7. Protocol for stressing mitochondria

Freshly isolated mitochondria were stressed by loading with 50 μM MCB, higher than the 20 μM MCB used for monitoring GSH. At 50 μM, MCB will partially deplete the available GSH pool without affecting

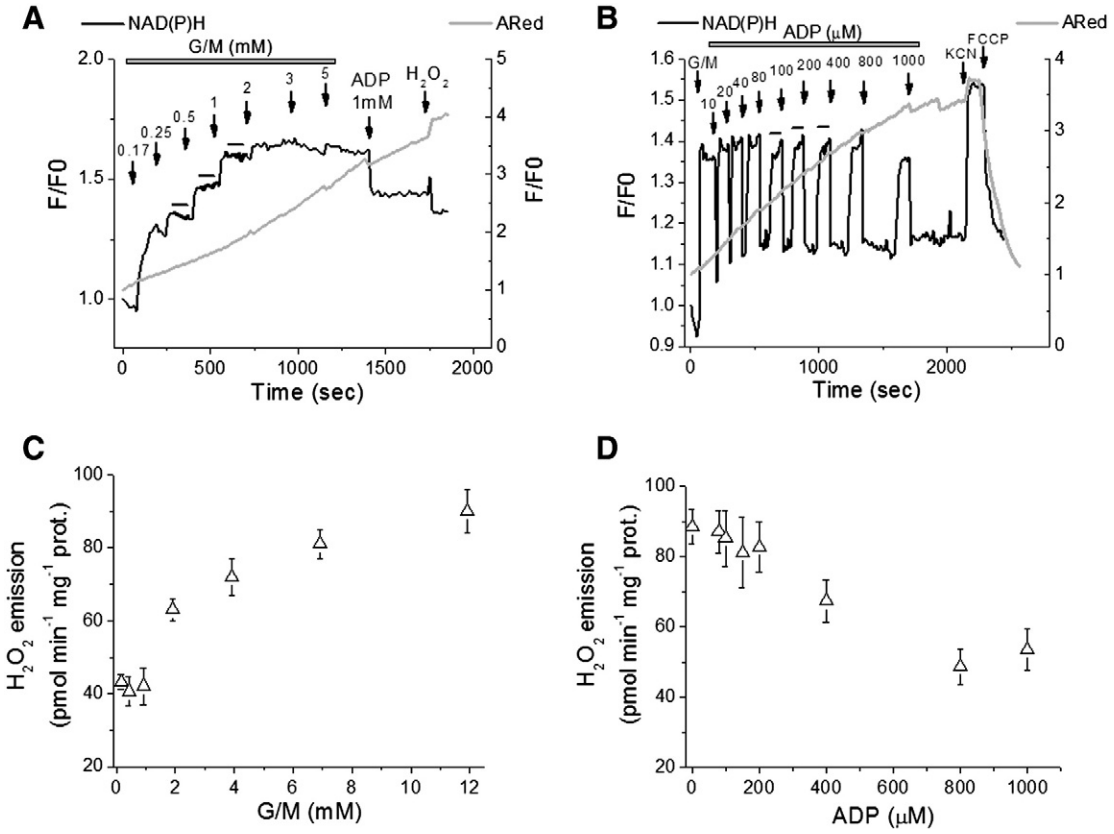

Fig. 2. Substrate-induced redox transitions under pseudo steady state conditions. Freshly isolated mitochondria from guinea pig heart were monitored simultaneously for NAD(P)H and H_2O_2 emission with Amplex Red [ARed] as a function of increasing concentrations of G/M [A] or ADP after energization with 5 mM G/M [B]. The concentration-response change in specific rate of H_2O_2 emission as a function of G/M [C] or ADP [D] was determined. Measurements of H_2O_2 were performed during the periods marked, as examples, by thickening of the NAD(P)H traces topped by short horizontal lines in panels A and B. These corresponded to the late phase of the ADP phosphorylation response. ROS emission levels below 80 μM ADP could not be accurately measured thus not represented in panel D. F/F0 represents the fluorescent signal normalized with respect to the initial fluorescence value, i.e. before substrate addition. At the end of the experiment, 50nM H_2O_2 (A) or 1 mM KCN and 6 μM FCCP (B) were added for calibrating the ARed and NAD(P)H signals, respectively. See M&M for further explanation.

respiration. In Figure S3 we show that within the range 20 to 50 μM MCB does not affect respiration, and in Fig. 5B that it partially depletes ~50% and ~25% the GSH and NAD(P)H pools, respectively [compare with Fig. 4B]. MCB [50 μM]-loaded mitochondria were further challenged by oxidative stress with 1 μM H_2O_2 when assayed in the fluorometer for energy/redox variables or for VO_2 determination, under otherwise identical conditions utilized for control, non-stressed, mitochondria.

3. Results

Two main postulates of the R-ORB hypothesis are: *i*) the extent of ROS imbalance depends on the RE, and *ii*) ROS levels attain a minimum when respiration is maximal and the RE exhibits intermediate values. ROS increase under more reducing (i.e. right arm in Fig. 1) or severe oxidizing conditions (i.e. left arm in Fig. 1) although by different mechanisms [16]. Since normal substrate consumption changes mitochondrial RE, in the first section we analyze the response of mitochondrial ROS emission as a function of substrate concentration.

4. Cyclic changes in the rate of H_2O_2 release from mitochondria during energetic transitions: pseudo steady state and time-dependent behavior

4.1. Pseudo steady state behavior

Mitochondria dynamically modulate matrix redox potential, membrane potential ($\Delta\Psi_m$), and the pH gradient across the inner membrane when supplied with substrates [21,28]. In de-energized (substrate-depleted) mitochondria, redox and electrochemical gradients can be increased in a graded manner in response to increasing concentrations of respiratory substrate (Figs. 2 and S1). Dissipation of $\Delta\Psi_m$ and a decrease in NADH redox potential occurs during ATP synthesis initiated by ADP, ion or metabolite transport, or activation of the ROS scavenging systems. In addition, oxidation of the main components of the antioxidant system (GSH/GSSG, TrxSH2/TrxSS) can occur if NADPH levels become limiting [21,24].

The relationship between mitochondrial NAD(P)H and H_2O_2 emission (Amplex Red [ARed] oxidation) with increasing concentrations of G/M in the absence of ADP is shown in Fig. 2. H_2O_2 emission increases more than two fold over the range of G/M from 0.17 to 12 mM [Fig. 2A and C].

Similarly, we challenged fully energized mitochondria in the presence of 5 mM G/M, with pulses of increasing ADP concentration. Fig. 2B shows that the NAD(P)H signal attains lower values concomitant to a decrease in the rate of change of ARed fluorescence as a function of increasing ADP. An almost linear decrease in H_2O_2 emission occurs as a function of ADP that levels off at 0.8 mM [Fig. 2D].

The results shown indicate that mitochondrial ROS emission augments or diminishes in parallel with a progressively more reduced or oxidized redox status as a function of G/M or G/M + ADP, respectively.

4.2. Time-dependent behavior

Fig. 3 depicts the phase relationship between different redox variables [NAD(P)H, GSH, ROS] during the state 4 → 3 transition elicited by successive ADP pulses. The mitochondrial energetic transition is clearly indicated by the orthodox → condensed shift in mitochondrial volume [29], as probed by 90° light scattering (LS) [19]. Following ADP addition, mitochondria contract (LS increases), and then swell again as ADP is consumed (LS decreases). Interestingly, the instantaneous rate of H_2O_2 emission (i.e. the first derivative [dARed/dt] of the ARed signal) decreases to a minimum at the peak of mitochondrial contraction and OxPhos rate, as indicated by NADH oxidation. The instantaneous rate of ROS release increases again when ADP is consumed

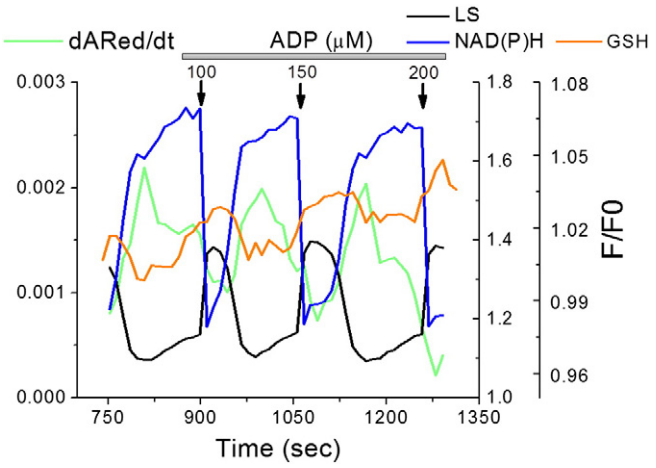

Fig. 3. Phase relationship between light scattering and redox variables during time-dependent redox/energetic transitions triggered by ADP pulses. Freshly isolated heart mitochondria from guinea pig were loaded with 20 μM MCB for GSH detection as described under M&M. MCB-loaded mitochondria [100–200 μg mitochondrial protein] were resuspended in a cuvette in the assay mixture described under M&M, energized with 5 mM G/M, and then subjected to pulses of increasing ADP concentration [from 10 μM to 800 μM]. Light scattering [LS], NAD(P)H, GSH, and the instantaneous rate of ROS emission [measured as the first derivative of the ARed signal, dARed/dt], were determined simultaneously. The axis for each variable is placed immediately below its corresponding label.

(Figs. 3 and S2), as can be judged from the mitochondrial increase in volume and NADH reduction.

We also monitored simultaneously the status of the GSH pool by loading mitochondria with the fluorescent probe MCB. Remarkably, the peak of GSH coincides with the minimum in H_2O_2 emission rate, which starts to decrease concomitantly with the rise of the ROS scavenger. The troughs in GSH reflect its maximal utilization during H_2O_2 scavenging. Electrons from NADH and Krebs cycle intermediates are not only directed to the respiratory chain but also to the scavenging systems, for example through pyridine nucleotide transhydrogenase activity and $NADP^+$-dependent isocitrate dehydrogenase to NADPH, which drives glutathione and thioredoxin reductases coupled to their respective peroxidases, glutathione peroxidase and peroxiredoxin [25,30,31].

Taken together, the data reveal that when mitochondria maximize their energetic output, ROS emission declines to a minimum, and increases thereafter as ADP is consumed. This behavior was verified both at pseudo steady state and during dynamic transitions in respiratory state.

5. ROS emission as a function of the RE

In the previous section, we showed that ROS release minima occur with more oxidized NAD(P)H redox state and high OxPhos rate, and that ROS flow increases under more reduced NAD(P)H redox states corresponding to low respiration both under steady (Fig. 2) and time-dependent (Fig. 3) states. Next, we determined H_2O_2 emission as a function of GSH and NAD(P)H that were monitored simultaneously to calculate the mitochondrial RE from these two major contributors.

Fig. 4 depicts the steady state levels of GSH and NAD(P)H as a function of G/M at state 4 respiration (no ADP added) [Fig. 4A] and at state 3 respiration with 5 mM G/M energized mitochondria challenged with consecutive pulses of increasing ADP concentration [Fig. 4B]. We can clearly see that ROS emission levels are augmented or diminished following a more reduced or oxidized RE elicited by G/M or ADP, respectively. H_2O_2 emission varies by approximately two-fold over the entire range of RE explored [Fig. 4C and D].

In terms of the R-ORB hypothesis, the data described above supports the relationship between ROS and RE on the right arm of the schematic plot displayed in Fig. 1, i.e., from intermediate to reduced values of the

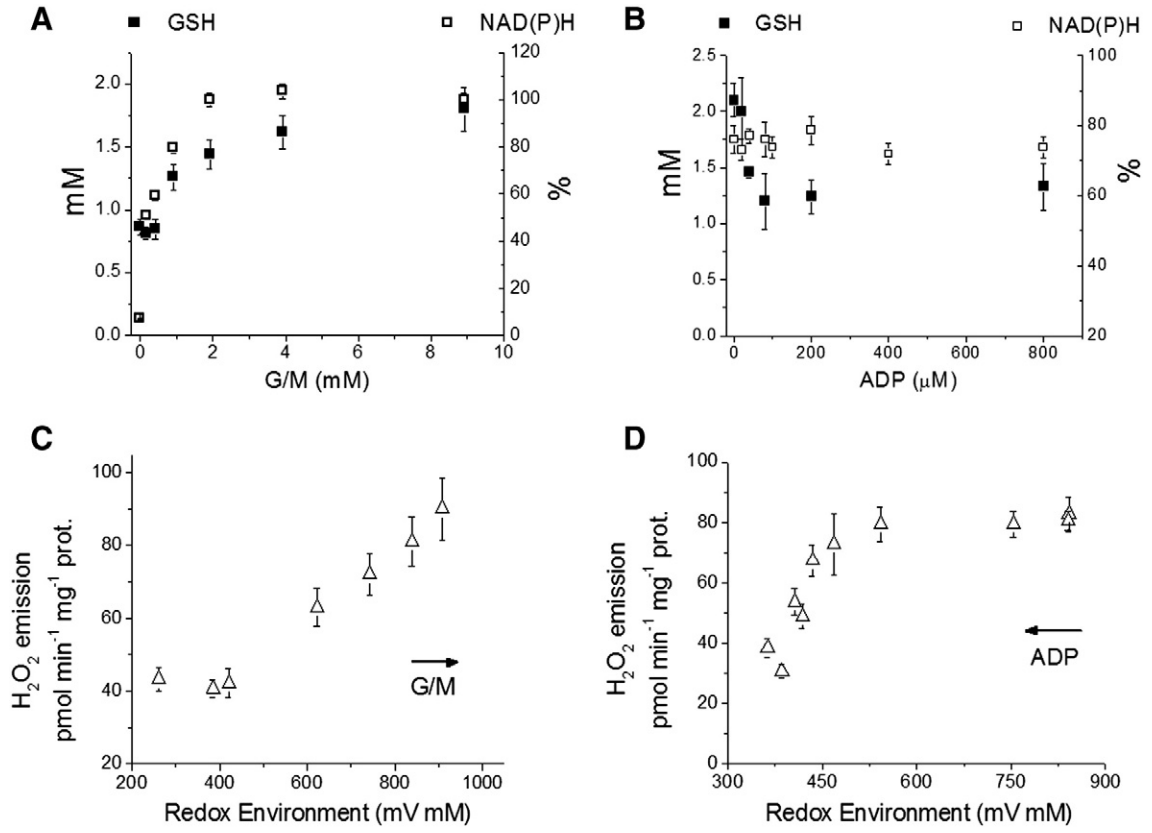

Fig. 4. RE as a function of substrate addition in non-stressed mitochondria. The experiment was carried out with MCB-loaded [20 μM] mitochondria as described in Fig. 3. The relative abundance of NAD(P)H (%) and GSH (mM) and H_2O_2 emission were monitored simultaneously as a function of G/M [A, state 4 respiration] or 5 mM G/M plus different concentrations of ADP [B, state 3 respiration], and the RE as a function of G/M [C] and ADP [D] calculated as described under M&M. From the data in panel B, the RE in the abscissa of panel D was calculated; the additional symbols in panel D correspond to interpolated values, e.g. GSH at 400 μM ADP. The NAD(P)H signal was calibrated as described under M&M. The arrows in panels C and D indicate increasing substrate addition.

RE. To explore this relationship under conditions in which the GSH pool is more oxidized, we stressed mitochondria by loading them with 50 μM MCB, which will partially deplete the available GSH pool without affecting respiration [see M&M]. Under conditions in which MCB-loaded mitochondria were further challenged by oxidative stress with 1 μM H_2O_2, ROS emission levels were about 2-fold higher than in non-stressed mitochondria in response to both G/M and ADP additions [compare panels C and D between Figs. 4 and 5]. ROS emission behaved independently from G/M but not from ADP levels, and remained at high levels over the range of G/M concentrations studied [Fig. 5C], but declined as ADP concentration increased [Fig. 5D]. Interestingly, the range of variation of the RE was larger in non-stressed as compared with stressed mitochondria (i.e. ~200 to ~900 vs. ~200 to ~550 mV·mM) (Figs. 4C, D and 5C, D). The difference in GSH level was the main underlying factor responsible for the relative oxidation of the mitochondrial RE under oxidative stress (compare panel B in Figs. 4 and 5).

The results indicate that under non-stressful conditions mitochondrial ROS emission levels exhibit a clear dependence on the RE in a certain range of values: from ~400 to ~900 mV·mM in state 4 respiration (Fig. 4C) and ~500 to ~300 mV·mM in state 3 respiration (Fig. 4D). However, under oxidative conditions, although mitochondrial ROS emission was high, it became independent of RE under state 4 and only weakly dependent on RE under state 3 respiration (Fig. 5C and D).

6. Respiration and ROS emission as a function of the RE

Concerning the central issue of the relationship between energetic and redox aspects of mitochondrial function, a main prediction of the R-ORB is that ROS emission levels will attain a minimum when mitochondrial energetic output is maximal [16]. We directly tested this proposal by assessing, in parallel, the rates of mitochondrial respiration [VO_2], ROS emission, and the RE.

Fig. 6 shows the behavior of VO_2 and H_2O_2 emission as a function of the RE varied as a function of ADP concentration. It can be clearly seen that H_2O_2 emission tends to lower values at maximal VO_2 [Fig. 6A]. The strong dependence of ROS emission on RE occurs in the restricted range comprised between ~500 and ~400 mV·mM, when respiratory flux is highest, remaining independent thereafter. This behavior reflects the prototypical flux (e.g. respiration, ATP synthesis) vs. force (e.g. RE, phosphorylation potential) relationship exhibited by energy transducers (see Discussion). As compared with non-stressed controls, stressed mitochondria displayed a similar dependence of H_2O_2 emission on the RE but in a significantly more oxidized range: ~300 and ~200 mV·mM and higher levels of ROS (~3-fold at maximal emission) [Fig. 6B].

We also evaluated the relationship between VO_2 and H_2O_2 emission vs. $\Delta\Psi_m$, under both non-stressed [Fig. 7A] and stressed [Fig. 7B] conditions. Under state 3 respiration, ROS emission varied 2- and 1.5-fold in a rather narrow ~7 mV span of $\Delta\Psi_m$ in control and stressed mitochondria, respectively. Likewise the RE, the dependence between ROS and $\Delta\Psi_m$ was strongest at maximal VO_2. Importantly, ROS emission was not sensitive to $\Delta\Psi_m$ changes within the range corresponding to state 4 respiration [Figs. 7A, B and S1, S5]. This observation is relevant because MU predicts that the sensitivity of H_2O_2 emission to $\Delta\Psi_m$ will be highest under state 4, when mitochondria are maximally energized.

Energetic performance, assessed by measuring VO_2 vs. ADP, was markedly altered in oxidatively stressed mitochondria as compared to control, non-stressed, mitochondria. V_{max} was 15% lower ($p < 0.05$ stressed vs. non-stressed), and the Km for ADP was non-significantly decreased [Fig. 6C, D; black data points], while uncoupled VO_2 [Fig. 6C

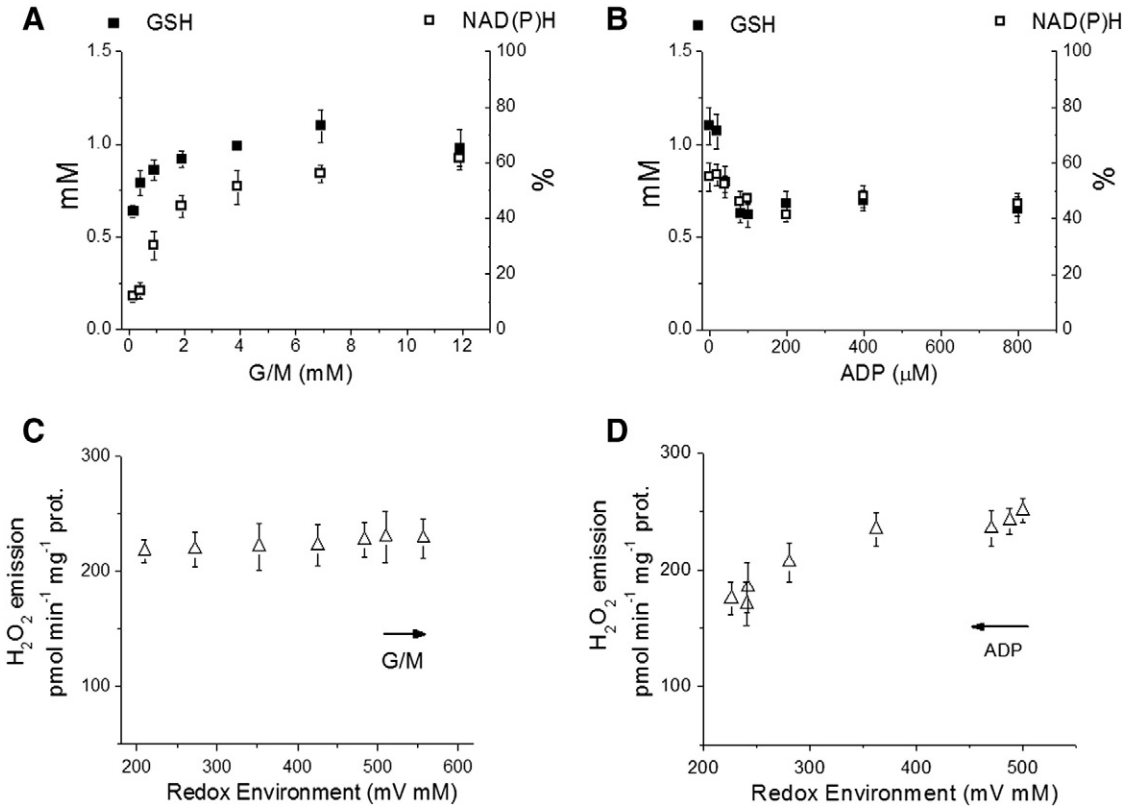

Fig. 5. RE as a function of substrate addition in stressed mitochondria. Mitochondria loaded with higher MCB concentration [50 μM] were assayed as described in Fig. 3 but further stressed with 1 μM H_2O_2 before starting the titration with substrates (see M&M). NAD(P)H and GSH abundance, H_2O_2 emission and the RE were determined as described in the legend of Fig. 4. The RE was estimated as described under M&M. The arrows in panels C and D indicate increasing substrate addition.

and D; empty circles] decreased by 33% in stressed mitochondria ($p < 0.01$ stressed vs. non-stressed).

Taken together, the data presented are in agreement with the idea that when mitochondrial respiration is maximal, ROS efflux is strongly dependent on RE and trends to a minimum. At respiratory rates below maximum, the dependence between ROS and the RE appears to be weaker. Although, in general, stressed mitochondria follow a similar behavior, the RE was significantly more oxidized, ROS levels were higher and respiration lower.

7. Discussion

The main contribution of this work is to show that mitochondria are able to maximize their energetic output while keeping ROS emission to a minimum. This major principle of R-ORB converges on the idea that mitochondria have evolved in such a way that optimization of redox and energetic functions concur [Fig. 6]. Under pseudo steady state and time-dependent conditions triggered by ADP pulses, the rate of ROS emission also decreases to a minimum at maximal rate of OxPhos [Fig. 3]. However, this capacity is partially lost under oxidative stress where mitochondria decrease their energetic output concomitantly with a more oxidized RE and increased ROS emission [Fig. 6]. R-ORB was initially postulated based on data obtained with guinea pig heart mitochondria, however we do not expect that this choice will influence the validity of the findings that we report herein as applied to other species [20].

The concerted actions of GSH/thioredoxin [Trx] scavenging systems in mitochondria are essential for keeping minimal levels of H_2O_2 emission, especially during state 3 respiration, when the energetic output is maximal [20]. The well-orchestrated function of the two antioxidant systems working continuously to offset ROS production is chiefly responsible for the minimum in ROS emission attained at intermediate values of RE and also for the inability of mitochondria to limit ROS overflow under stressful oxidant conditions. State 3 respiration transients, induced by ADP additions, show that minima in the rate of H_2O_2 emission occur concomitantly with increase in the GSH fluorescence signal. Apparently, this response of the GSH pool [Fig. 3] differs from the global decrease in GSH observed during state 3 respiration by direct assay in mitochondrial supernatants [Fig. 4B]. A possible explanation would be that MCB, the fluorescent probe of GSH, is reporting a local pool of this molecule, different from the bulk phase. A drop in the dynamic balance between the rate of ROS production by the respiratory chain and the rate of ROS scavenging under maximal OxPhos, may explain a transient recovery of the local GSH pool reported by the probe.

8. Mitochondrial ROS emission and redox-energy transduction under normal and stressful conditions

The dependence of mitochondrial ROS efflux on the RE follows the general sigmoidal-curve shape exhibited by energy transducers, i.e. quasi linear flux-force relation within a certain span, and independence at extreme low or high values of the driving force [32]. The range where ROS and RE exhibit dependence is wider under state 4 than state 3 respiration for non-stressed mitochondria (Fig. 4C and D). However, under stress, mitochondria display H_2O_2 emission levels about 2-fold higher than in its absence (compare Figs. 4C, D and 5C, D), and exhibit no relation (Fig. 5C) or a weak one (Fig. 5D) between ROS vs. RE (Fig. 5C and D). Apparently, oxidative stress shifts the RE toward the more oxidized range where the ROS efflux is insensitive to the RE in state 4 (compare Figs. 4C and 5C) and less sensitive in state 3 respiration (compare Figs. 4D and 5D). A decrease in mitochondrial matrix GSH of ~50% is mainly responsible for the shift (compare Figs. 4B and 5B) and the higher ROS emission, i.e. reduced antioxidant capacity. Understanding the energetic and redox behavior of mitochondria under oxidative stress is a significant biological problem because of the increasingly recognized fact that aging and chronic diseases such as diabetes and

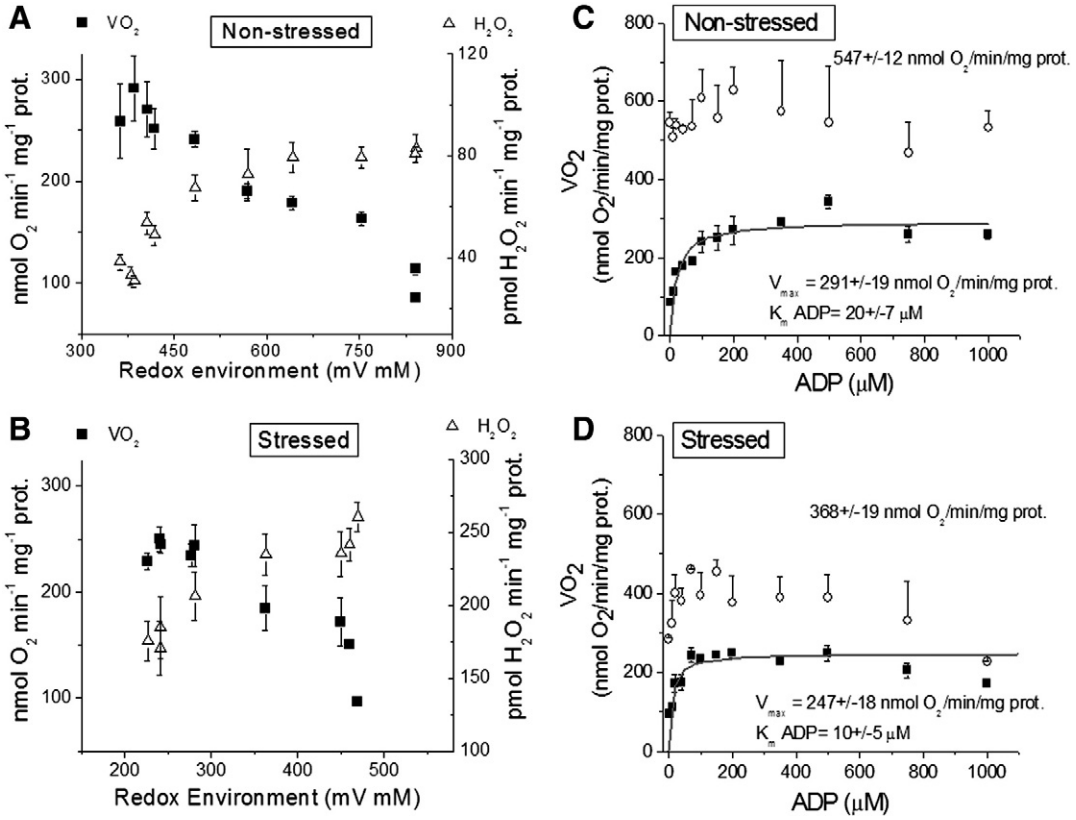

Fig. 6. Mitochondrial respiration and H_2O_2 emission as a function of RE. Mitochondria loaded with 20 μM MCB concentration [non-stressed: A, C] or 50 μM MCB plus 1 μM H_2O_2 addition [stressed: B, D] were assayed in parallel for redox variables [NAD(P)H, GSH, H_2O_2] by fluorometry [A, B] and respiration, VO_2 [C, D] as a function of ADP concentration (from 10 to 800 μM) with high throughput Seahorse equipment as described [see M&M]. In panels C and D displayed are the state 3 [black squares] and uncoupled with 50 μM dinitrophenol [empty circles] VO_2 values. The RE determined from GSH and NAD(P)H was calculated as described under M&M.

obesity involve the progressive deterioration of the redox status of cells and the organism [9,22,33].

Concerning energetics, the respiratory flux was lower under oxidative stress than in its absence (Fig. 6A and B) although $\Delta\Psi_m$ was similar (Fig. S1A and C). The latter result suggests that the NADH-electron-donor capacity to respiration might have been diminished under stress likely due to redirection of electrons to the antioxidant systems. Indeed, the relationship between respiration and ROS is altered by oxidative stress, resulting in decreased mitochondrial energetic performance and higher levels of ROS emission (Figs. 6–8).

Present data suggest that under high energy demand, e.g. exercise, in the absence of additional oxidative stress, mitochondria will function at relatively more reduced RE, i.e. from right arm to the minimum ROS rather than on the left arm [Figs. 1 and 8]. However, a shift to more oxidized REs will happen under pathological conditions thus displacing mitochondrial function toward the left arm of the plot in Fig. 1 (see Fig. 8). This was indeed the case for heart mitochondria isolated from diabetic guinea pigs as shown by recent data from our laboratory (Tocchetti, Stanley, Sivakumaran, O'Rourke, Paolocci, Cortassa, Aon, submitted). Likewise, an effective shift to higher ROS release was observed previously [16], when heart mitochondria were stressed under similar conditions and were subjected to increasing levels of uncoupling (thick gray arrow pointing toward the dash-dot line in Fig. 8). In fact, the redox stress introduced by FCCP in already stressed mitochondria [Fig. S3 A and B] was responsible for further RE oxidation and higher ROS emission [16].

9. Role of compartmentation and the release of ROS from mitochondria

As redox/energetic functions of mitochondria are intermingled, so are the mitochondrial and cytoplasmic REs. A dynamic interaction between the mitochondrial RE and energetic function may underlie mitochondrial dysfunction in aging and disease. For instance, in burn injury, mitochondrially targeted antioxidant treatment with the peptide SS-31 improves mitochondrial redox status, restoring OxPhos coupling and ATP synthesis rate in skeletal muscle [34].

As a dynamic metric, the RE is a function of the different redox couples accounting for both their redox potential and the concentration of the reduced species [21,22]. The RE exhibits its own dynamics in different but interdependent cellular compartments, e.g. mitochondria and cytoplasm, mediated by exchange of ROS and redox-related components such as GSH. Compartmentation plays a significant role in the control of ROS levels, the RE, and dynamic behavior [21]. Furthermore, and since GSH/Trx scavenging systems appear to act concertedly and continuously to keep low rates of H_2O_2 emission from mitochondria [20], duplication of antioxidant defense systems in multiple compartments can be viewed as an efficient salvage mechanism to avoid or to reduce oxidative bursts [21].

The phenomenological concept of "mitohormesis" refers to the association observed between increased mitochondrial metabolism and ROS formation with the induction of an adaptive response that culminates in increased stress resistance, antioxidant defense and extended life span [35,36]. This concept is similar to what R-ORB proposes as levels of ROS compatible with physiological signaling, due to moderate increases around the minimum toward more reduced or oxidized RE [see Fig. 1, gray area around the minimum]. Conceptually, mitohormesis points out that not all increase in ROS is negative, but it can be positive instead. However, mitohormesis does not specify under which conditions the adaptive response will happen, and how this is compatible with mitochondria supplying energy reliably and consistently, while at the same time keeping ROS levels within non detrimental boundaries compatible with physiological signaling.

10. The intermediary between respiration and ROS

Considering the role of $\Delta\Psi_m$ and RE as intermediaries between mitochondrial respiration and ROS, we should keep in mind that redox and energetic functions are inextricably linked. An example is NADH and its electron-donating role to both the respiratory chain and the antioxidant systems through transhydrogenase conversion into NADPH. Electric [$\Delta\Psi_m$] and redox [NADH] potentials build up after G/M addition to non-energized mitochondria, and are dissipated following ADP addition [Figs. S1 and S5]. One could argue that electric and redox potentials could both explain mitochondrial ROS modulation, since they are difficult to untangle. However, the following arguments favor RE over $\Delta\Psi_m$ as a candidate intermediate between respiration and ROS. First, ROS emission levels varied strongly as a function of the RE over a 200 mV·mM range, in part due to the 20 mV drop in the redox potential of GSH:GSSG [Fig. 6], whereas $\Delta\Psi_m$ only changed 7 mV for the same span [Fig. 7]. A larger rather than a narrow range of variation in a control parameter is more in agreement with the robust function of a system. According to R-ORB, mitochondria optimize both maximal energetic output and minimum ROS emission, thus a co-variation of ROS and $\Delta\Psi_m$ is expected at maximal VO_2 [Fig. 7]. Second, as a driving force, the RE accounts both for ROS production in the respiratory chain and the ROS scavenging capacity of mitochondria, while $\Delta\Psi_m$ only accounts for changes in ROS production. Third, in state 4 respiration, the condition under which MU was formulated, no modification in ROS emission occurs for a similar range of variation in $\Delta\Psi_m$ of ~6 mV when compared to state 3 respiration [Figs. 7, S1, and S5]. This important observation indicates that the shape of the relationship between ROS emission and RE or $\Delta\Psi_m$ is dependent upon the type of intervention, i.e. exponential with uncouplers [14,16,17], or sigmoidal-shaped with natural substrates (G/M, ADP) as described herein.

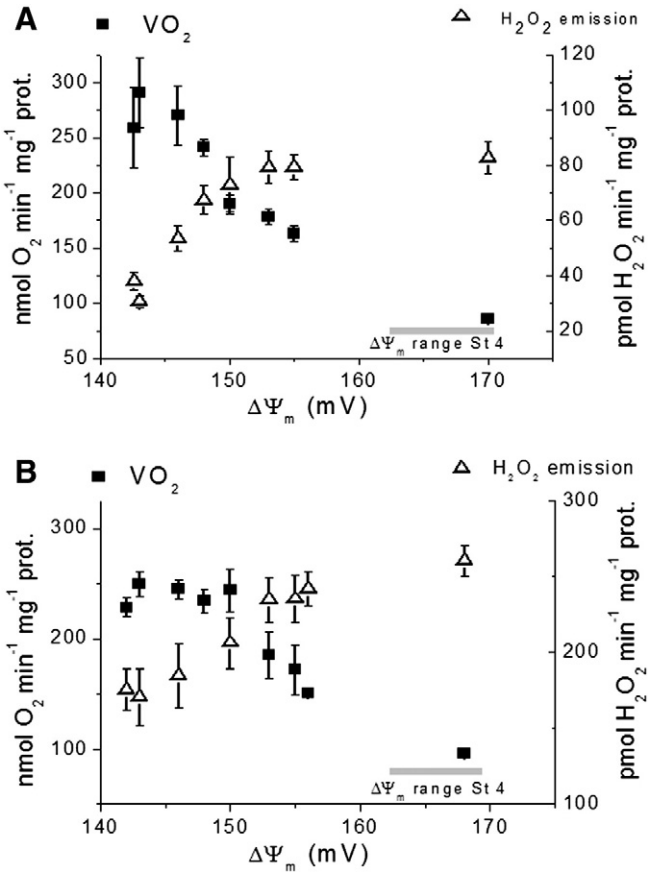

Fig. 7. Mitochondrial respiration and H_2O_2 emission as a function of $\Delta\Psi_m$. Experiments were performed as described in the legend of Fig. 6 and the data for non-stressed (A) and stressed (B) mitochondria represented as a function of $\Delta\Psi_m$ that was monitored simultaneously with NAD(P)H and GSH, and in parallel with H_2O_2 or respiration. See Figure S5 for a representative experiment where $\Delta\Psi_m$ can be monitored at state 4 and 3 respirations.

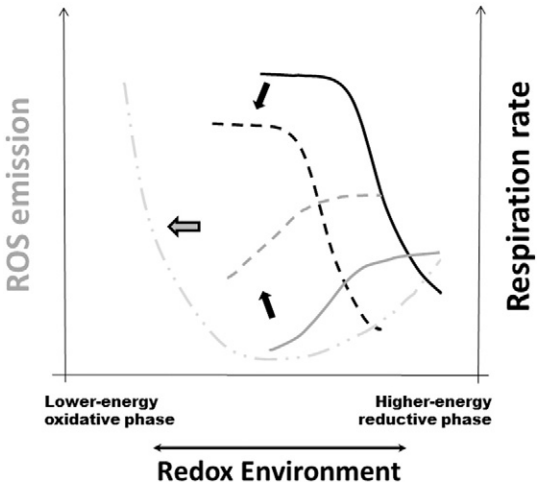

Fig. 8. Effect of oxidative stress on mitochondrial respiration, H_2O_2 emission, and RE. The plot displays the summary of the response of respiration (black traces) and ROS emission in mitochondria stressed with MCB and exogenously added H_2O_2 (gray traces) plus further addition of the uncoupler FCCP (dashed-dotted line). Continuous lines correspond to the absence of stress whereas dashed lines belong to mitochondria under stressed conditions. Black arrows indicate the direction of change in VO_2 and ROS elicited by stress. Notice the shift toward more oxidized RE in the curves corresponding to stressful conditions. The thick gray arrow pointing to the left denotes pathological conditions arising, e.g. from chronic diseases, where severe stress will affect both energetic (e.g. $\Delta\Psi_m$, ADP consumption) and redox (e.g. NAD(P)H, GSH, Trx) functions thus increased mitochondrial ROS emission and higher cytoplasmic ROS levels [37].

11. Conclusions

Defining the relationship between mitochondrial respiration and ROS emission is crucial to understanding compatibility between reliable energy supply, minimization of oxidative damage, and ROS signaling. In the framework of the R-ORB hypothesis, this work tested the critical idea of whether the RE or $\Delta\Psi_m$ is the main intermediary between respiration and ROS under normal and stressful conditions. The main finding shows that ROS emission is a strong function of the RE, which works as a robust and encompassing controller of both production and scavenging of ROS. The evidence presented supports the idea that the R-ORB hypothesis, in terms of optimization, reconciles maximal energetic output with minimal ROS likely compatible with signaling.

We conclude that conceptually R-ORB offers a broader framework for describing the relationship between respiration and ROS, since it may account for both physiological and pathological conditions, while including MU as a special case under certain conditions, i.e. the behavior corresponding to the right hand arm of the plot in Fig. 1.

Acknowledgements

This work was supported by NIH grants R01-HL091923-01 [MAA], R21HL106054 [SC], R37HL054598 and R01HL105216 [BO'R].

Appendix A. Supplementary data

Supplementary data to this article can be found online at http://dx.doi.org/10.1016/j.bbabio.2013.11.007.

References

[1] A.K. Camara, M. Bienengraeber, D.F. Stowe, Mitochondrial approaches to protect against cardiac ischemia and reperfusion injury, Front. Physiol. 2 (2011) 13.
[2] A.K. Camara, E.J. Lesnefsky, D.F. Stowe, Potential therapeutic benefits of strategies directed to mitochondria, Antioxid. Redox Signal. 13 (2010) 279–347.

[3] I. Bratic, A. Trifunovic, Mitochondrial energy metabolism and ageing, Biochim. Biophys. Acta 1797 (2010) 961–967.
[4] M.M. Sedensky, P.G. Morgan, Mitochondrial respiration and reactive oxygen species in mitochondrial aging mutants, Exp. Gerontol. 41 (2006) 237–245.
[5] H. Bugger, E.D. Abel, Mitochondria in the diabetic heart, Cardiovasc. Res. 88 (2010) 229–240.
[6] U.E. Martinez-Outschoorn, F. Sotgia, M.P. Lisanti, Power surge: supporting cells "fuel" cancer cell mitochondria, Cell Metab. 15 (2012) 4–5.
[7] D.C. Wallace, Mitochondria and cancer, Nat. Rev. Cancer 12 (2012) 685–698.
[8] P. Helguera, J. Seiglie, J. Rodriguez, M. Hanna, G. Helguera, J. Busciglio, Adaptive downregulation of mitochondrial function in down syndrome, Cell Metab. 17 (2013) 132–140.
[9] F.G. Akar, M.A. Aon, G.F. Tomaselli, B. O'Rourke, The mitochondrial origin of postischemic arrhythmias, J. Clin. Invest. 115 (2005) 3527–3535.
[10] M.A. Aon, S. Cortassa, F.G. Akar, B. O'Rourke, Mitochondrial criticality: a new concept at the turning point of life or death, Biochim. Biophys. Acta 1762 (2006) 232–240.
[11] B. O'Rourke, S. Cortassa, M.A. Aon, Mitochondrial ion channels: gatekeepers of life and death, Physiology (Bethesda) 20 (2005) 303–315.
[12] K.H. Fisher-Wellman, P.D. Neufer, Linking mitochondrial bioenergetics to insulin resistance via redox biology, Trends Endocrinol. Metab. 23 (2012) 142–153.
[13] M.D. Brand, Uncoupling to survive? The role of mitochondrial inefficiency in ageing, Exp. Gerontol. 35 (2000) 811–820.
[14] S.S. Korshunov, V.P. Skulachev, A.A. Starkov, High protonic potential actuates a mechanism of production of reactive oxygen species in mitochondria, FEBS Lett. 416 (1997) 15–18.
[15] V.P. Skulachev, Role of uncoupled and non-coupled oxidations in maintenance of safely low levels of oxygen and its one-electron reductants, Q. Rev. Biophys. 29 (1996) 169–202.
[16] M.A. Aon, S. Cortassa, B. O'Rourke, Redox-optimized ROS balance: a unifying hypothesis, Biochim. Biophys. Acta 1797 (2010) 865–877.
[17] A.A. Starkov, "Mild" uncoupling of mitochondria, Biosci. Rep. 17 (1997) 273–279.
[18] A.A. Starkov, G. Fiskum, Regulation of brain mitochondrial H_2O_2 production by membrane potential and NAD(P)H redox state, J. Neurochem. 86 (2003) 1101–1107.
[19] M.A. Aon, S. Cortassa, A.C. Wei, M. Grunnet, B. O'Rourke, Energetic performance is improved by specific activation of K^+ fluxes through K(Ca) channels in heart mitochondria, Biochim. Biophys. Acta 1797 (2010) 71–80.
[20] M.A. Aon, B.A. Stanley, V. Sivakumaran, J.M. Kembro, B. O'Rourke, N. Paolocci, S. Cortassa, Glutathione/thioredoxin systems modulate mitochondrial H2O2 emission: an experimental-computational study, J Gen Physiol 139 (2012) 479–491.
[21] J.M. Kembro, M.A. Aon, R.L. Winslow, B. O'Rourke, S. Cortassa, Integrating mitochondrial energetics, redox and ROS metabolic networks: a two-compartment model, Biophys. J. 104 (2013) 332–343.
[22] F.Q. Schafer, G.R. Buettner, Redox environment of the cell as viewed through the redox state of the glutathione disulfide/glutathione couple, Free Radic. Biol. Med. 30 (2001) 1191–1212.
[23] A.G. Cox, C.C. Winterbourn, M.B. Hampton, Mitochondrial peroxiredoxin involvement in antioxidant defence and redox signalling, Biochem. J. 425 (2010) 313–325.
[24] B.A. Stanley, V. Sivakumaran, S. Shi, I. McDonald, D. Lloyd, W.H. Watson, M.A. Aon, N. Paolocci, Thioredoxin reductase-2 is essential for keeping low levels of H(2)O(2) emission from isolated heart mitochondria, J. Biol. Chem. 286 (2011) 33669–33677.
[25] M.A. Aon, S. Cortassa, C. Maack, B. O'Rourke, Sequential opening of mitochondrial ion channels as a function of glutathione redox thiol status, J. Biol. Chem. 282 (2007) 21889–21900.
[26] S. Cortassa, M.A. Aon, R.L. Winslow, B. O'Rourke, A mitochondrial oscillator dependent on reactive oxygen species, Biophys. J. 87 (2004) 2060–2073.
[27] M.K. Slodzinski, M.A. Aon, B. O'Rourke, Glutathione oxidation as a trigger of mitochondrial depolarization and oscillation in intact hearts, J. Mol. Cell. Cardiol. 45 (2008) 650–660.
[28] A.C. Wei, M.A. Aon, B. O'Rourke, R.L. Winslow, S. Cortassa, Mitochondrial energetics, pH regulation, and ion dynamics: a computational-experimental approach, Biophys. J. 100 (2011) 2894–2903.
[29] C.R. Hackenbrock, Chemical and physical fixation of isolated mitochondria in low-energy and high-energy states, Proc. Natl. Acad. Sci. U. S. A. 61 (1968) 598–605.
[30] J.B. Hoek, J. Rydstrom, Physiological roles of nicotinamide nucleotide transhydrogenase, Biochem. J. 254 (1988) 1–10.
[31] L.A. Sazanov, J.B. Jackson, Proton-translocating transhydrogenase and NAD- and NADP-linked isocitrate dehydrogenases operate in a substrate cycle which contributes to fine regulation of the tricarboxylic acid cycle activity in mitochondria, FEBS Lett. 344 (1994) 109–116.
[32] H.V. Westerhoff, K. Van Dam, Thermodynamics and Control of Biological Free-Energy Transduction, Elsevier, Amsterdam, 1987.
[33] W. Droge, Free radicals in the physiological control of cell function, Physiol. Rev. 82 (2002) 47–95.
[34] V. Righi, C. Constantinou, D. Mintzopoulos, N. Khan, S.P. Mupparaju, L.G. Rahme, H.M. Swartz, H.H. Szeto, R.G. Tompkins, A.A. Tzika, Mitochondria-targeted antioxidant promotes recovery of skeletal muscle mitochondrial function after burn trauma assessed by in vivo 31P nuclear magnetic resonance and electron paramagnetic resonance spectroscopy, FASEB J 27 (2013) 2521–2530.
[35] E.J. Calabrese, Hormesis and medicine, Br. J. Clin. Pharmacol. 66 (2008) 594–617.
[36] M. Ristow, K. Zarse, How increased oxidative stress promotes longevity and metabolic health: the concept of mitochondrial hormesis (mitohormesis), Exp. Gerontol. 45 (2010) 410–418.
[37] C.G. Tocchetti, V. Caceres, B.A. Stanley, C. Xie, S. Shi, W.H. Watson, B. O'Rourke, R.C. Spadari-Bratfisch, S. Cortassa, F.G. Akar, N. Paolocci, M.A. Aon, GSH or palmitate preserves mitochondrial energetic/redox balance, preventing mechanical dysfunction in metabolically challenged myocytes/hearts from type 2 diabetic mice, Diabetes 61 (2012) 3094–3105.